

Abstract

In-situ observations of atmospheric CO₂ and O₂ concentrations at Hateruma Island (HAT, 24° N, 124° E) often show synoptic scale pollution events when air masses are transported from East Asian source regions. We calculate the regression slopes (-ΔO₂/ΔCO₂ molar ratios) of the correlation plots between O₂ and CO₂ for selected pollution events observed between October 2006 and December 2008. The observed -ΔO₂/ΔCO₂ ratios vary from 1.0 to 1.7. Categorizing the air mass origins for the pollution events by using back trajectory analysis, we find that there is a significant difference in the average -ΔO₂/ΔCO₂ ratios between events from China (1.14±0.12, *n* = 25) and Japan/Korea (1.37±0.15, *n* = 16). These values are comparable to the -O₂:CO₂ molar exchange ratios, which are estimated from the national fossil fuel inventories from CDIAC. Simulations using a particle dispersion model reveal that the pollution events at HAT are predominantly CO₂ emissions from the combustion of fossil fuels in East Asian countries, which is consistent with the above observational results. Although the average value of the model-predicted -ΔO₂/ΔCO₂ ratios for Japan/Korea origin is underestimated in comparison with the observation, that for China origin agree well with the observation. The sensitivity experiment suggests that the -ΔO₂/ΔCO₂ ratio at HAT reflects about 90% of the change in the -O₂:CO₂ exchange ratio for the fossil carbon emissions from China.

1 Introduction

There is a tight negative stoichiometric coupling between oxygen (O₂) flux and carbon dioxide (CO₂) flux of land biotic respiration and photosynthesis processes and burning processes of fossil fuels and biomass. The -O₂:CO₂ molar exchange ratios are different for the land biotic and burning processes because the ratio is basically dependent on the elemental compositions of related organic and inorganic matters. Keeling (1988) estimated the -O₂:CO₂ ratios for coal, liquid fuel, and natural gas burning to

Atmospheric O₂ and CO₂ changes of pollution events in East Asia

C. Minejima et al.

Title Page

Abstract

Introduction

Conclusions

References

Tables

Figures

⏪

⏩

◀

▶

Back

Close

Full Screen / Esc

Printer-friendly Version

Interactive Discussion



be 1.17 ± 0.03 , 1.44 ± 0.03 and 1.95 ± 0.04 , respectively. The estimated global average $-\text{O}_2:\text{CO}_2$ molar exchange ratio for land biotic processes is 1.10 ± 0.05 (Severinghaus, 1995). On the other hand, an analogous stoichiometric coupling between O_2 and CO_2 fluxes for air-sea gas exchange processes does not exist because oceanic CO_2 flux is significantly suppressed by a chemical equilibrium between dissolved CO_2 , bicarbonate and carbonate ions.

The O_2 and CO_2 fluxes from land biotic and burning processes should cause the correlative changes in the atmospheric concentrations of O_2 and CO_2 downwind of the source region. Recent improvements in O_2 measurement technique have enabled the detection of high-frequency changes in atmospheric O_2 concentrations simultaneously with that of CO_2 (Manning et al., 1999; Stephens et al., 2003; Yamagishi et al., 2008) and the $-\Delta\text{O}_2/\Delta\text{CO}_2$ changing ratios for such pollution events have recently been used to constrain the contributions from individual sources. For example, Stephens et al. (2003) conducted continuous in situ measurements of O_2 and CO_2 on research cruises in the equatorial Pacific and Southern Oceans and found that some short-term variations were caused by the combustion of liquid fossil fuels. Stephens et al. (2007) also found clearly different $-\Delta\text{O}_2/\Delta\text{CO}_2$ ratios corresponding to the land biotic exchange and fossil fuel burning in short-term atmospheric O_2 and CO_2 variations over a forest canopy at the WLEF tall-tower research site in Northern Wisconsin. In addition, Lueker et al. (2001) examined the varying $-\Delta\text{O}_2/\Delta\text{CO}_2$ ratio in short-term CO_2 and O_2 variations at Trinidad Head when the observations were influenced from wildfire emissions and discuss the relationship between the ratio and wildfire dynamics.

The National Institute for Environmental Studies (NIES) has been measuring atmospheric O_2 and CO_2 by flask sampling at Hateruma Island (HAT, 24°N , 124°E) since July, 1997 at a frequency of several flasks per month (Tohjima et al., 2003; Tohjima et al., 2008). To capture more frequent O_2 variations, we started in-situ O_2 measurements at HAT from October 2006. The prevailing wind direction in winter time is northwest due to the East Asian monsoon. Therefore, the observations at HAT often show pollution events influenced by emissions from East Asian countries from the late fall to early

Atmospheric O_2 and CO_2 changes of pollution events in East Asia

C. Minejima et al.

[Title Page](#)[Abstract](#)[Introduction](#)[Conclusions](#)[References](#)[Tables](#)[Figures](#)[⏪](#)[⏩](#)[◀](#)[▶](#)[Back](#)[Close](#)[Full Screen / Esc](#)[Printer-friendly Version](#)[Interactive Discussion](#)

spring each year (Tohjima et al., 2002; Yokouchi et al., 2006; Tohjima et al., 2010). This setting gives us a unique opportunity to analyze the relation between O_2 and CO_2 variations in the pollution events with respect to the East Asian source regions.

In this manuscript, we investigate the $-\Delta O_2/\Delta CO_2$ ratios for the pollution events observed at HAT. Source regions of the individual pollution events are distinguished by back trajectory analysis, and the observed $-\Delta O_2/\Delta CO_2$ ratios are compared with the calculated $-O_2:CO_2$ ratios based on reported compositions of the fossil fuel types at their air mass origins. In addition, we analyze the contribution of regional emissions and the individual sources to the observed O_2 and CO_2 changes, and we adopt atmospheric transport models based on a Lagrangian particle dispersion model, FLEXPART (Stohl et al., 1998), and conduct comparisons between the observation and the model simulation.

2 Observation data and analytical methods

2.1 Observation at HAT

HAT is a small elliptical (longer in the east-west direction) island with an area of 12.7 km^2 and a population of 600, and is located at the southern edge of Japanese archipelago. The monitoring station is situated on the eastern edge of the island, and the prevailing wind direction at the station is northerly in winter and southerly in summer. Local emissions from the island were determined to be not a significant influence on the observations at HAT.

The air is sampled from an inlet at the height of 36.5 m on a tower (46.5 m above sea level) at a flow rate of about 9 STP L/min by a diaphragm pump (MOA-P108-HB, Gast Mfg. Corp., Benton Harbor, MI, USA). The air intake is covered with an inverted circular cylinder (diameter: 10 cm, height: 15 cm) and the sampling line is composed of a 1/2 inch OD stainless steel tubing. The sampled air is then introduced into the O_2/N_2 measurement system including a gas chromatograph equipped with a thermal

Atmospheric O_2 and CO_2 changes of pollution events in East Asia

C. Minejima et al.

Title Page

Abstract

Introduction

Conclusions

References

Tables

Figures

⏪

⏩

◀

▶

Back

Close

Full Screen / Esc

Printer-friendly Version

Interactive Discussion



conductivity detector (GC/TCD). Details of sampling, analyzing and data processing methods are described elsewhere (Tohjima, 2000; Yamagishi et al., 2008). The CO₂ concentrations are continuously measured by a nondispersive infrared analyzer (NDIR) (Mukai et al., 2001).

Changes in O₂ concentration are expressed as a relative deviation of the O₂/N₂ ratio from an arbitrary reference according to

$$\delta(\text{O}_2/\text{N}_2) = [(\text{O}_2/\text{N}_2)_{\text{sample}}/(\text{O}_2/\text{N}_2)_{\text{reference}} - 1] \times 10^6. \quad (1)$$

Following Keeling and Shertz (1992), we use the units of “per meg” to express the $\delta(\text{O}_2/\text{N}_2)$ value. A value of 4.8 per meg is equivalent to the mole fraction of 1 $\mu\text{mol mol}^{-1}$ (ppm) in a trace gas abundance. Here, the $\delta(\text{O}_2/\text{N}_2)$ values are determined against our original reference scale (Tohjima et al., 2008). The O₂/N₂ ratio was measured every 10 min and the standard deviation of the O₂/N₂ ratio measurement is estimated to be ± 14 per meg (~ 3 ppm), thus has a standard error of ± 6 per meg (~ 1.2 ppm) for an one-hour average. The CO₂ values are reported on the NIES gravimetric standard scales (NIES-09) based on the CO₂-in-air standard gases prepared by gravimetric one-step dilution method (Machida et al., 2011). The CO₂ analytical precision is about 0.1 ppm.

In this study, we analyze the hourly O₂/N₂ ratios and CO₂ mixing ratios observed during the period from October 2006 to December 2008 (Fig. 1). The observed CO₂ clearly shows secular increasing trend and seasonal cycle with an increase in the fall and winter and decrease in the spring and summer, while the observed O₂/N₂ shows the opposite trend and seasonal cycle. Besides these relatively long-term variations, the CO₂ and O₂/N₂ show the short-term variations with the synoptic time scales associated with the pollution events especially in the late fall to early spring.

2.2 Correlation analysis of pollution events

In order to extract the short-term variation components of CO₂ and O₂/N₂, we first obtain smooth-curve fits to the data following the methods of Thoning et al. (1989) with

Atmospheric O₂ and CO₂ changes of pollution events in East Asia

C. Minejima et al.

Title Page

Abstract

Introduction

Conclusions

References

Tables

Figures

⏪

⏩

◀

▶

Back

Close

Full Screen / Esc

Printer-friendly Version

Interactive Discussion



a cut-off frequency of 4.6 cycles yr^{-1} (see Fig. 1), and then subtract the smooth-curve fits from the original time series. The extracted short-term variations are denoted by the Δ notation as ΔCO_2 and ΔO_2 .

Hourly ΔCO_2 and ΔO_2 measurements over a one-month period (7 November to mid 22 December 2007) are shown in Fig. 2a and 2b, respectively. From these short-term variations, we identified pollution events as follows. First, we found largely varying ΔCO_2 events where the difference between the maximum and minimum is larger than 4.1 ppm (twice the standard deviation of whole ΔCO_2) and the duration ranged from 12-h to 3-days. It should be noted that the start and end times of events are determined by peak like variations by visual inspection. Then the correlation coefficient (r) between ΔO_2 and ΔCO_2 variations and the linear regression slope ($-\Delta\text{O}_2/\Delta\text{CO}_2$ ratio) are computed for each event. For the following analysis, we discarded events with $|r| < 0.8$. Adopting this criterion, we eliminated about 40% of the pollution events and in total, we analyzed 67 pollution events in the followings. For example, we identified three pollution events during the 1-month period as shown in Fig. 2.

We categorize the origins of the pollution events into 3 regions: China, Japan/Korea and other, using a kinematic 5-day back trajectory calculated by the METEX (METeoro-logical data Explorer, <http://db.cger.nies.go.jp/metex/>) (Zeng et al., 2003). Altitude of the starting point for the calculation is set at 40 m above ground level, which is close with the altitude of the sample inlet. Arrival time of each air mass corresponds to the time when the highest CO_2 concentration in each event is observed.

In the back trajectory calculations, the National Center for Environmental Prediction (NCEP) reanalysis data with a time resolution of 6 h, latitude/longitude grid of 2.5 degree and 17 pressure levels are used (Kistler et al., 2001). The first country to intersect the back trajectory is assigned as the origin of the air mass. Among the 67 pollution events, 25 and 16 events are assigned to China and Japan/Korea origins, respectively. Figure 3 shows all resulting trajectories assigned to China and Japan/Korea as their origins with four events assigned to other as examples.

Atmospheric O_2 and CO_2 changes of pollution events in East Asia

C. Minejima et al.

Title Page

Abstract

Introduction

Conclusions

References

Tables

Figures

⏪

⏩

◀

▶

Back

Close

Full Screen / Esc

Printer-friendly Version

Interactive Discussion

2.3 Model simulation

2.3.1 Lagrangian Particle Dispersion Model (LPDM), FLEXPART

In order to investigate the influence of regional fluxes and the contributions of individual flux categories to the pollution events, a Lagrangian particle dispersion model, FLEXPART v3.2 (Stohl et al., 1998), is used in this study. FLEXPART calculates the trajectories of multiple tracer particles using mean winds interpolated from the meteorological fields and random motions representing turbulences. Three-hourly meteorology data from Global Forecast System (GFS) provided by the National Center for Environmental Prediction (NCEP) are used as the meteorological fields, which have a spatial resolution of $1^\circ \times 1^\circ$. In each simulation, 10,000 particles are released from a receptor position (the inlet of the tower at HAT in this study) and transported eight days backward in time. The time step of the calculation is 900 s and each transported particle absorbs the CO_2 and O_2 fluxes ($\text{kg m}^{-2} \text{ day}^{-1}$) of its location once a day when it is located under the altitude of 1000 m. Changing the criterion altitude where the particles absorb the fluxes from 300 m to 2000 m, we found no significant difference in resultant CO_2 concentrations. At last, CO_2 and O_2 fluxes each particle absorbed are summed and concentrations were calculated using the method developed by Seibert and Frank (2004). The CO_2 and O_2 concentration changes calculated this way include the influence of fluxes and meteorology for the previous eight days, which gives enough time for particles to spread over the East Asia.

The CO_2 flux from fossil fuel burning and cement production (FFB&C) was produced based on the flux used in TransCom model simulation, fossil98 (Law et al., 2008). The flux was originally made from the Carbon Dioxide Information Analysis Center's (CDIAC) national total of the year 1998 (Marland et al., 2003) and spatial distribution by $1^\circ \times 1^\circ$ EDGAR (Olivier and Berdowski, 2001). FFB&C was prepared for each year and was kept constant throughout the year. This fossil98 was modified so that the national totals of the top 20 CO_2 emitting countries match the emissions of that year (Marland et al., 2007). In order to make the CO_2 flux from FFB&C for the year 2008, the increase

15637

Atmospheric O_2 and CO_2 changes of pollution events in East Asia

C. Minejima et al.

Title Page

Abstract

Introduction

Conclusions

References

Tables

Figures

⏪

⏩

◀

▶

Back

Close

Full Screen / Esc

Printer-friendly Version

Interactive Discussion



rates from 2006 to 2007 for the top 20 countries were used. The biospheric CO₂ uses optimized CASA flux (Nakatsuka and Maksyutov, 2009) and oceanic component is air-sea CO₂ flux from Takahashi et al (2002). The biospheric and oceanic fluxes are available monthly and they are converted into daily fluxes through linear interpolation.

The O₂ fluxes from FFB&C was produced by multiplying the CO₂ flux from FFB&C by the -O₂:CO₂ exchange ratios calculated by the corresponding fuel compositions. The national -O₂:CO₂ ratios of 1.11, 1.37, and 1.31 for China, Japan and Korea, respectively, are used for the fluxes in 2006. For the remaining countries, a single -O₂:CO₂ ratio, 1.45, based on the average fuel compositions of these remaining countries is used to produce the O₂ fluxes. Similarly, the O₂ fluxes from the terrestrial biosphere (TB) are prepared as a product of the optimized CASA flux and the land biotic -O₂:CO₂ exchange ratio of 1.1. For O₂ flux from ocean, we use the monthly mean climatological oceanic fluxes of Garcia and Keeling (2001).

2.3.2 The global coupled Eulerian-Lagrangian transport model (the coupled model)

The atmospheric CO₂ and O₂ changes predicted by FLEXPART only reflect the regional fluxes within the range of locations of dispersed particles for up to eight days in this study. In order to include larger scale background influence, we also use a global coupled Eulerian-Lagrangian transport model (coupled model) developed by Koyama et al. (2011). It is comprised of a global Eulerian transport model, the NIES-TM (Maksyutov et al., 2008), and a regional LPDM, FLEXPART. The NIES-TM component gives the initial concentration of the air mass eight days in the past, and FLEXPART gives the eight days plume transport for 10 000 particles. The CO₂ concentrations simulated by NIES-TM at the location of each particle at eight days back is averaged to predict the influence of the background CO₂ concentration. The same flux set that was used for FLEXPART was used for the coupled model. NIES-TM is driven by JCDAS-25 and is run with a horizontal resolution of 2.5°×2.5°, with 15 sigma levels. JCDAS-25 has a time resolution of 12-h and a spatial resolution of 2.5°×2.5°.

Atmospheric O₂ and CO₂ changes of pollution events in East Asia

C. Minejima et al.

Title Page

Abstract

Introduction

Conclusions

References

Tables

Figures

⏪

⏩

◀

▶

Back

Close

Full Screen / Esc

Printer-friendly Version

Interactive Discussion



3 Results and discussion

3.1 Observed $-\Delta\text{O}_2/\Delta\text{CO}_2$ ratios

The $-\Delta\text{O}_2/\Delta\text{CO}_2$ ratios for the observed pollution events categorized as the China and Japan/Korea origins are shown in Fig. 4a, in which the ratios are collapsed into a single year. Although the $-\Delta\text{O}_2/\Delta\text{CO}_2$ ratios for both events show large variability with a range from 1.0 to 1.7, the range for China origin tends to be lower (1.0–1.4) than the latter (1.1–1.7). Therefore, the average $-\Delta\text{O}_2/\Delta\text{CO}_2$ ratios are 1.14 ± 0.12 for China and 1.37 ± 0.15 for Japan/Korea, respectively (uncertainties given here are 1σ standard deviations). The Welch's t-test reveals that the average of the $-\Delta\text{O}_2/\Delta\text{CO}_2$ ratios between China and Japan/Korea events differ with more than a 99.9% confidence level. For comparison, we also calculate the average $-\text{O}_2:\text{CO}_2$ exchange ratios of FFB&C for China and Japan/Korea using the 2006 national fossil carbon inventories provided by CDIAC (Boden et al., 2010) and the $-\text{O}_2:\text{CO}_2$ molar exchange ratios for individual fuel types (Keeling, 1988). The calculated $-\text{O}_2:\text{CO}_2$ exchange ratios are 1.11 ± 0.03 for China and 1.34 ± 0.02 for Japan/Korea, which show excellent agreements with the above average $-\Delta\text{O}_2/\Delta\text{CO}_2$ values for the observed pollution events from the corresponding regions. These values are summarized in Table 1 and are plotted in Fig. 5. It should be noted that the higher percentage of the CO_2 emissions from coal burning and cement manufacturing for China results in a significantly lower $-\text{O}_2:\text{CO}_2$ ratio of 1.11 in comparison with Japan and Korea. Note that, the $-\text{O}_2:\text{CO}_2$ ratio associated with cement manufacturing is zero because CO_2 emission from it does not involve O_2 consumption.

These results suggest that the observed air masses arriving at Hateruma predominantly reflect the characteristics of CO_2 emission and O_2 consumption from fossil fuel burning at their source regions, and that land biotic and oceanic fluxes contribute little to the observed O_2 and CO_2 variations in these pollution events.

3.2 Simulated $-\Delta O_2/\Delta CO_2$ ratios

Figure 2 also shows the time series of the hourly ΔCO_2 and ΔO_2 data simulated by FLEXPART and the coupled model. The model results generally well reproduce the observed pollution events. However, precise comparisons reveal that there are often differences in the phase and size between the simulated and observed CO_2 and O_2 short-term variations associated with the pollution events. Therefore, the simulated pollution events whose phases are off by more than 10 h and whose sizes are less than 1.4 ppm (twice the standard deviation of whole modeled ΔCO_2) are discarded in the following analysis. Using these criteria, we obtain 27 pollution events (14 China events and 13 Japan/Korea events) by the FLEXPART and the coupled model simulations. Note that all the correlation coefficients for the simulated CO_2 and O_2 variations of the selected 27 pollution events are larger than 0.8.

Figure 4b shows the $-\Delta O_2/\Delta CO_2$ ratios calculated by FLEXPART and the coupled model for the 27 selected events. In general, the $-\Delta O_2/\Delta CO_2$ ratios of FLEXPART and the coupled models agree well with each other although the Japan/Korea events in February and March show slightly different $-\Delta O_2/\Delta CO_2$ ratios between the two models.

Figure 6 shows a scatter plot of the $-\Delta O_2/\Delta CO_2$ ratios simulated by FLEXPART versus the observed ratios. The model-simulated $-\Delta O_2/\Delta CO_2$ ratios do not necessarily reconstruct the individual observed ratios. When all events in Fig. 6 are taken as a group, a high correlation is not seen. However, upon examining the relationships for the China events and Japan/Korea events separately, we find significant correlation for the Japan/Korea events with a correlation coefficient (r) of 0.79 and a regression slope of 0.71. On the other hand, both the observed and simulated $-\Delta O_2/\Delta CO_2$ ratios of China events have small variations and are clustered around 1.1.

The averages of the $-\Delta O_2/\Delta CO_2$ ratios for the model predictions together with those of observations are also summarized in Table 1 and are plotted in Fig. 5. The averages of the observed and simulated $-\Delta O_2/\Delta CO_2$ ratios for the China events agree well with a 95 % confidence level (Welch's t-test). Other the other hand, for the Japan/Korea

Atmospheric O_2 and CO_2 changes of pollution events in East Asia

C. Minejima et al.

Title Page

Abstract

Introduction

Conclusions

References

Tables

Figures

⏪

⏩

◀

▶

Back

Close

Full Screen / Esc

Printer-friendly Version

Interactive Discussion

events the simulated $-\Delta\text{O}_2/\Delta\text{CO}_2$ ratios are significantly lower than those of the observation with the same confidence level. Some of the average $-\Delta\text{O}_2/\Delta\text{CO}_2$ ratios from the model predictions are slightly smaller than the land biotic $-\text{O}_2:\text{CO}_2$ exchange ratio of 1.1. This is mostly due to ocean fluxes because we find that removing the oceanic CO_2 and O_2 components brings those averages closer to 1.10.

The simulated $-\Delta\text{O}_2/\Delta\text{CO}_2$ ratios by FLEXPART and the coupled model for the China events are very close to each other. Although the average values of the simulated $-\Delta\text{O}_2/\Delta\text{CO}_2$ ratios by FLEXPART and the coupled model for the Japan/Korea events show a small difference, but it is not significant with the 95 % confidence level from the Welch's t-test. These results suggest that the background influence to the $-\Delta\text{O}_2/\Delta\text{CO}_2$ ratio for the pollution events is relatively small.

4 Discussion

As described in the previous section, there are excellent agreements between the observed $-\Delta\text{O}_2/\Delta\text{CO}_2$ ratios and the calculated $-\text{O}_2:\text{CO}_2$ exchange ratios based on the fossil fuel statistics for China and Japan/Korea. This result suggests that the pollution events at HAT are predominantly due to FFB&C fluxes and that contributions from land biotic and oceanic fluxes are relatively small. To examine the contributions of individual flux components in short-term variations, the ΔCO_2 components derived from FFB&C, TB and ocean are depicted in Fig. 7, which shows that most of the peaks come from FFB&C emissions. That is due to CO_2 fluxes of FFB&C at the grids corresponding to urban areas, which are generally an order of magnitude larger than their TB CO_2 fluxes and two orders of magnitude larger than oceanic ingassing fluxes (CO_2 is absorbed slightly by the ocean in the marginal region of the East Asia at this time of year). In addition, the predominant contribution of FFB&C to the predicted pollution event is due to the more localized nature of CO_2 emissions from FFB&C in highly populated areas, whereas TB CO_2 emission is rather widely distributed over the country with little spatial variability. Thus, FFB&C CO_2 appears as peaks while TB CO_2 is smeared as

Atmospheric O_2 and CO_2 changes of pollution events in East Asia

C. Minejima et al.

Title Page

Abstract

Introduction

Conclusions

References

Tables

Figures

⏪

⏩

◀

▶

Back

Close

Full Screen / Esc

Printer-friendly Version

Interactive Discussion



background.

In order to elucidate that FFB&C is the main contributor to the modeled $-\Delta\text{O}_2/\Delta\text{CO}_2$ ratio and not the fluxes from TB, two sensitivity tests are performed. First, a FLEXPART model simulation is performed in which the land biotic $-\text{O}_2:\text{CO}_2$ ratio changed from 1.1 to 1.0, and the $-\Delta\text{O}_2/\Delta\text{CO}_2$ ratios are recalculated. This brings the average $-\Delta\text{O}_2/\Delta\text{CO}_2$ ratio for China events from 1.08 to 1.05, while the average $-\Delta\text{O}_2/\Delta\text{CO}_2$ ratio for Japan/Korea events stayed at 1.09. Second, the national $-\text{O}_2:\text{CO}_2$ ratio for China is changed from 1.11 to 1.00 and O_2 fluxes from FFB&C is prepared with the ratio. Then $-\Delta\text{O}_2/\Delta\text{CO}_2$ ratios were recalculated after the FLEXPART model simulation. This brings the average $-\Delta\text{O}_2/\Delta\text{CO}_2$ for China and Japan/Korea from 1.08 to 0.98 and 1.09 to 1.06, respectively. The results of these two experiments confirm that the average $-\Delta\text{O}_2/\Delta\text{CO}_2$ for China is much more sensitive than the Chinese national $-\text{O}_2:\text{CO}_2$ ratio than to the land biotic $-\text{O}_2:\text{CO}_2$ exchange.

On the other hand, the average predicted $-\Delta\text{O}_2/\Delta\text{CO}_2$ for Japan/Korea events is also affected by the national $-\text{O}_2:\text{CO}_2$ ratio of China while it is insensitive to the value of the land biotic exchange ratio. It is consistent with the rather low value of the predicted $-\Delta\text{O}_2/\Delta\text{CO}_2$ for Japan/Korea. It suggests that the contribution of emissions from China to the pollution events assigned as Japan/Korea is overestimated in the model simulations and about 50 % of FFB&C CO_2 contribution on average comes from China.

Figure 8 shows footprints of representative pollution events. Figure 8a is an event assigned to China. Figure 8b and c are events assigned to Japan/Korea which has small and large Chinese influence, respectively. The footprint [g-C m^{-3}] is defined as a product of the ratio of particle number in a grid in the set mixed layer height to the total particle number [no unit], the residence time [day], and the anthropogenic FFB&C CO_2 flux [$\text{g-C m}^{-2} \text{ day}$] divided by a set mixing layer height, 1000m. Thus, those grids, which have large flux and particle numbers, have large contribution to the observed signal at HAT. Figure 8a shows a footprint of air masses observed at Hateruma for the period of 04:00–22:00 LT on 3 March 2008. METEX analysis designates the air mass is from China and that is confirmed by its footprint. Figure 8b shows a footprint observed

Atmospheric O_2 and CO_2 changes of pollution events in East Asia

C. Minejima et al.

Title Page

Abstract

Introduction

Conclusions

References

Tables

Figures



Back

Close

Full Screen / Esc

Printer-friendly Version

Interactive Discussion



at Hateruma for the period of 02:00 LT, 6 November–09:00, 7 November 2007. Back trajectory analysis shows the origin to be Japan/Korea and in this case the strongest influence comes from megacities in Japan. While back trajectories suggest the origins of the events to be Japan/Korea, in many cases, however, the footprint covers not only Japan/Korea but also China. Such an example is shown in Fig. 8c, where a footprint for the time period from 01:00 on 14 March to 14:00 on 15 March 2008 is depicted. In this case, contribution of emissions from China is about 81 % of the pollution event in the FLEXPART simulation.

In the FLEXPART simulation, pollution events categorized as Japan/Korea in origin by the back trajectory analysis almost always contains substantial contribution of Chinese fluxes and the average $-\Delta\text{O}_2/\Delta\text{CO}_2$ value is closer to that of China. One possibility is that particle spread in the simulation seems to be wider than that in reality. One solution for both problems would be to use higher spatially and temporally resolved meteorological fields. Another approach is to use more spatially resolved fluxes. In order to better reproduce the observed events, how the model is set up to absorb flux can be improved, especially the treatment of the planetary boundary layer.

5 Conclusion

We examined the correlation between changes in atmospheric O_2 and CO_2 concentrations for selected pollution events observed at HAT between October 2006 and December 2008. The regression slopes ($-\Delta\text{O}_2/\Delta\text{CO}_2$ molar ratios) for these pollution events showed large variability with a range of 1.0 to 1.7. Based on the 5-day back trajectories calculated with METEX, the origins of the pollution events were categorized into 3 regions: China, Japan/Korea and other. We found that there was a significant difference in the average $-\Delta\text{O}_2/\Delta\text{CO}_2$ ratio between China (1.14 ± 0.12) and Japan/Korea (1.37 ± 0.15) origins. These values are comparable to the $-\text{O}_2:\text{CO}_2$ exchange ratios, which are estimated from the national fossil fuel inventories for the corresponding countries. The results suggest that the atmospheric O_2 and CO_2 measurements combined

Atmospheric O_2 and CO_2 changes of pollution events in East Asia

C. Minejima et al.

Title Page

Abstract

Introduction

Conclusions

References

Tables

Figures



Back

Close

Full Screen / Esc

Printer-friendly Version

Interactive Discussion



with back trajectory analysis could be used to constrain the compositions of fuel types from regional emissions.

Using a particle dispersion model (FLEXPART) and a global coupled Eulerian-Lagrangian transport model (the coupled model), we simulated the atmospheric CO₂ and O₂ changes at HAT. In these simulations, O₂ and CO₂ fluxes from FFB&C, TB, and ocean were adopted. The simulated results generally reconstruct the atmospheric O₂ and CO₂ variations associated with the pollution events. Analysis of the contribution of individual CO₂ fluxes to the atmospheric variations revealed that the most of the peaks associated with pollution events at HAT are attributed to FFB&C CO₂ emissions. The average $-\Delta O_2/\Delta CO_2$ ratios of the 14 predicted pollution events from China, which were well reproduced by FLEXPART and the coupled model, agreed well with the average of the observed $-\Delta O_2/\Delta CO_2$ ratios. The additional sensitivity analysis showed that the predicted $-\Delta O_2/\Delta CO_2$ ratio for China was substantially sensitive to the change in the $-O_2:CO_2$ exchange ratio of FFB&C for China and reflected the change by 90%. These results suggest that the observed $-\Delta O_2/\Delta CO_2$ ratios at HAT would be able to detect changes in the composition of fossil fuel types used in China.

On the other hand, model simulations underestimated the average $-\Delta O_2/\Delta CO_2$ for the Japan/Korea pollution events. This is probably due to the larger contribution of emissions from China to the Japan/Korea pollution events at HAT in the model simulations. At the same time, there is little difference between FLEXPART and the coupled model, indicating that the influence of the background O₂ and CO₂ changes to the $-\Delta O_2/\Delta CO_2$ ratios for the pollution events are relatively small.

Acknowledgements. We are grateful to Nobukazu Oda of the Global Environmental Forum and local staffs for continuously supporting our in situ measurements. We also thank Toshinobu Machida and Kei-ichi Katsumata for determining CO₂ concentrations of the reference gases used at HAT and Shigeru Hashimoto for data processing of CO₂. We are grateful to Andreas Stohl for providing the FLEXPART model code. The datasets, JCDAS-25, used for this study are provided from the cooperative research project of the JRA-25 long-term reanalysis by the Japan Meteorological Agency (JMA) and the Central Research Institute of Electric Power Industry (CRIEPI). This work was financially supported by the Ministry of the Environment through the

Atmospheric O₂ and CO₂ changes of pollution events in East Asia

C. Minejima et al.

Title Page

Abstract

Introduction

Conclusions

References

Tables

Figures



Back

Close

Full Screen / Esc

Printer-friendly Version

Interactive Discussion



References

- 5 Boden, T. A., Marland, G., and Andres, R. J.: Global, Regional, and National Fossil-Fuel CO₂ Emissions, Carbon Dioxide Information Analysis Center, Oak Ridge National Laboratory, US Department of Energy, Oak Ridge, Tenn., USA, doi:10.3334/CDIAC/00001_V2010, available online at: http://cdiac.ornl.gov/trends/emis/tre_glob.html, last access: 19 May 2011, 2009.
- Garcia, H. E. and Keeling, R. F.: On the global oxygen anomaly and air-sea flux, *J. Geophys. Res.-Ocean.*, 106, 31155–31166, 2001.
- 10 Gregg, J. S., Andres, R. J., and Marland, G.: China: Emissions pattern of the world leader in CO₂ emissions from fossil fuel consumption and cement production, *Geophys. Res. Lett.*, 35, L08806, doi:10.1029/2007GL032887, 2008.
- Keeling, R. F.: Development of an interferometric oxygen analyzer for precise measurement of the atmospheric O₂ mole fraction, Ph.D., Harvard Univ., Cambridge, Mass., USA, 178 pp., 15 1988.
- Keeling, R. F. and Shertz, S. R.: Seasonal and interannual variations in atmospheric oxygen and implications for the global carbon-cycle, *Nature*, 358, 723–727, 1992.
- Kistler, R., Kalnay, E., Collins, W., Saha, S., White, G., Woollen, J., Chelliah, M., Ebisuzaki, W., Kanamitsu, M., Kousky, V., van den Dool, H., Jenne, R., and Fiorino, M.: The NCEP-NCAR 20 50-year reanalysis: Monthly means CD-ROM and documentation, *B. Am. Meteorol. Soc.*, 82, 247–267, 2001.
- Koyama, Y., Maksyutov, S., Mukai, H., Thoning, K., and Tans, P.: Simulation of variability in atmospheric carbon dioxide using a global coupled Eulerian-Lagrangian transport model, *Geosci. Model Dev.*, 4, 317–324, doi:10.5194/gmd-4-317-2011, 2011.
- 25 Law, R. M., Peters, W., Rodenbeck, C., Aulagnier, C., Baker, I., Bergmann, D. J., Bousquet, P., Brandt, J., Bruhwiler, L., Cameron-Smith, P. J., Christensen, J. H., Delage, F., Denning, A. S., Fan, S., Geels, C., Houweling, S., Imasu, R., Karstens, U., Kawa, S. R., Kleist, J., Krol, M. C., Lin, S. J., Lokupitiya, R., Maki, T., Maksyutov, S., Niwa, Y., Onishi, R., Parazoo, N., Patra, P. K., Pieterse, G., Rivier, L., Satoh, M., Serrar, S., Taguchi, S., Takigawa, M., Vautard, R., Vermeulen, A. T., and Zhu, Z.: Transcom model simulations of hourly atmospheric 30

Atmospheric O₂ and CO₂ changes of pollution events in East Asia

C. Minejima et al.

Title Page

Abstract

Introduction

Conclusions

References

Tables

Figures



Back

Close

Full Screen / Esc

Printer-friendly Version

Interactive Discussion



Atmospheric O₂ and CO₂ changes of pollution events in East Asia

C. Minejima et al.

Title Page

Abstract

Introduction

Conclusions

References

Tables

Figures

◀

▶

◀

▶

Back

Close

Full Screen / Esc

Printer-friendly Version

Interactive Discussion

CO₂: Experimental overview and diurnal cycle results for 2002, *Global Biogeochem. Cy.*, 22, GB3009, doi:10.1029/2007gb003050, 2008.

Lueker, T. J., Keeling, R. F., and Dubey, M. K.: The oxygen to carbon dioxide ratios observed in emissions from a wildfire in northern California, *Geophys. Res. Lett.*, 28, 2413–2416, 2001.

5 Machida, T., Tohjima, Y., Katsumata, K., and Mukai, H.: A new CO₂ calibration scale based on gravimetric one-step dilution cylinders in National Institute for Environmental Studies-NIES 09 CO₂ scale, in: Report of the 15th WMO Meeting of Experts on Carbon Dioxide Concentration and Related Tracer Measurement Techniques, Jena, Germany, 7–10 September 2009, WMO/GAW Rep. 194, edited by: Brand, W., 114–118, WMO, Geneva, Switzerland, 2011.

10 Maksyutov, S., Patra, P. K., Onishi, R., Saeki, T., and Nakazawa, T.: NIES/FRCGC global atmospheric tracer transport model: description, validation, and surface sources and sinks inversion, *J. Earth Sim.*, 9, 3–18, 2008.

Manning, A. C., Keeling, R. F., and Severinghaus, J. P.: Precise atmospheric oxygen measurements with a paramagnetic oxygen analyzer, *Global Biogeochem. Cy.*, 13, 1107–1115, 1999.

15 Marland, G., Boden, T. A., and Andres, R. J.: Global, regional, and national annual CO₂-emissions from fossil-fuel burning, cement production, and gas flaring: 1751–2002, NDP-030, Carbon Dioxide Inf. Anal. Cent., Oak Ridge Natl. Lab., <http://cdiac.esd.ornl.gov/ndps/ndp030.html>, last access: 19 May 2011, 2003.

20 Marland, G., Boden, T. A., and Andres, R. J.: Global, regional, and national CO₂ emissions, Carbon Dioxide Inf. Anal. Cent., Oak Ridge Natl. Lab., US Dept. Of Energy, Oak Ridge, Tenn., USA, 2007.

Marland, G. and Rotty, R. M.: Carbon-dioxide emissions from fossil-fuels - a procedure for estimation and results for 1950–1982, *Tellus B*, 36, 232–261, 1984.

25 Mukai, H., Katsumoto, M., Ide, R., Machida, T., Fujinuma, Y., Nojiri, Y., Inagaki, M., Oda, N., and Watai, T.: Characterization of atmospheric CO₂ observed at two-background air monitoring stations (Hateruma and Ochi-ishi) in Japan, Extended Abstract, Sixth International Carbon Dioxide Conference, 2–4 November 2011, Vol. I, 108–111, 2001.

30 Nakatsuka, Y. and Maksyutov, S.: Optimization of the seasonal cycles of simulated CO₂ flux by fitting simulated atmospheric CO₂ to observed vertical profiles, *Biogeosciences*, 6, 2733–2741, doi:10.5194/bg-6-2733-2009, 2009.

Olivier, J. G. J. and Berdowski, J. J. M.: Global emissions sources and sinks, *The Climate System*, edited by: Berdowski, J., Guicherit, R., and Heij, B. J., A. A. Balkema Publishers/Swets

Atmospheric O₂ and CO₂ changes of pollution events in East Asia

C. Minejima et al.

Title Page

Abstract

Introduction

Conclusions

References

Tables

Figures

⏪

⏩

◀

▶

Back

Close

Full Screen / Esc

Printer-friendly Version

Interactive Discussion



and Zeitlinger Publishers, Lisse, The Netherlands, 33–78, 2001.

Seibert, P. and Frank, A.: Source-receptor matrix calculation with a Lagrangian particle dispersion model in backward mode, *Atmos. Chem. Phys.*, 4, 51–63, doi:10.5194/acp-4-51-2004, 2004.

5 Severinghaus, J. P.: Studies of the terrestrial O₂ and carbon cycles in sand dune gases and in Biosphere, Ph.D., Columbia Univ., New York, NY, USA, 148 pp., 1995.

Stephens, B. B., Keeling, R. F., and Paplawsky, W. J.: Shipboard measurements of atmospheric oxygen using a vacuum-ultraviolet absorption technique, *Tellus B*, 55, 857–878, 2003.

10 Stephens, B. B., Bakwin, P. S., Tans, P. P., Teclaw, R. M., and Baumann, D. D.: Application of a differential fuel-cell analyzer for measuring atmospheric oxygen variations, *J. Atmos. Ocean. Tech.*, 24, 82–94, 2007.

Stohl, A., Hittenberger, M., and Wotawa, G.: Validation of the Lagrangian particle dispersion model FLEXPART against large-scale tracer experiment data, *Atmos. Environ.*, 32, 4245–4264, 1998.

15 Takahashi, T., Sutherland, S. C., Sweeney, C., Poisson, A., Metz, N., Tilbrook, B., Bates, N., Wanninkhof, R., Feely, R. A., Sabine, C., Olafsson, J., and Nojiri, Y.: Global sea-air CO₂ flux based on climatological surface ocean pCO₂, and seasonal biological and temperature effects, *Deep-Sea Res. Pt. II*, 49, 1601–1622, 2002.

20 Thoning, K. W., Tans, P. P., and Komhyr, W. D.: Atmospheric Carbon-Dioxide at Mauna Loa Observatory 2. Analysis of the NOAA GMCC Data, 1974–1985, *J. Geophys. Res.-Atmos.*, 94, 8549–8565, 1989.

Tohjima, Y.: Method for measuring changes in the atmospheric O₂/N₂ ratio by a gas chromatograph equipped with a thermal conductivity detector, *J. Geophys. Res.-Atmos.*, 105, 14575–14584, 2000.

25 Tohjima, Y., Machida, T., Utiyama, M., Katsumoto, M., Fujinuma, Y., and Maksyutov, S.: Analysis and presentation of in situ atmospheric methane measurements from cape Ochi-ishi and Hateruma island, *J. Geophys. Res.-Atmos.*, 107, 4148, doi:10.1029/2001jd001003, 2002.

Tohjima, Y., Mukai, H., Machida, T., and Nojiri, Y.: Gas-chromatographic measurements of the atmospheric oxygen/nitrogen ratio at Hateruma island and cape Ochi-ishi, Japan, *Geophys. Res. Lett.*, 30, 1653, doi:10.1029/2003GL017282, 2003.

30 Tohjima, Y., Mukai, H., Nojiri, Y., Yamagishi, H., and Machida, T.: Atmospheric O₂/N₂ measurements at two Japanese sites: Estimation of global oceanic and land biotic carbon sinks and analysis of the variations in atmospheric potential oxygen (APO), *Tellus B*, 60, 213–225,

2008.

Tohjima, Y., Mukai, H., Hashimoto, S., and Patra, P. K.: Increasing synoptic scale variability in atmospheric CO₂ at Hateruma island associated with increasing east-Asian emissions, *Atmos. Chem. Phys.*, 10, 453–462, doi:10.5194/acp-10-453-2010, 2010.

5 Yamagishi, H., Tohjima, Y., Mukai, H., and Sasaoka, K.: Detection of regional scale sea-to-air oxygen emission related to spring bloom near Japan by using in-situ measurements of the atmospheric oxygen/nitrogen ratio, *Atmos. Chem. Phys.*, 8, 3325–3335, doi:10.5194/acp-8-3325-2008, 2008.

10 Yokouchi, Y., Taguchi, S., Saito, T., Tohjima, Y., Tanimoto, H., and Mukai, H.: High frequency measurements of HFCs at a remote site in east Asia and their implications for Chinese emissions, *Geophys. Res. Lett.*, 33, L21814, doi:10.1029/2006gl026403, 2006.

Zeng, J. Y., Tohjima, Y., Fujinuma, Y., Mukai, H., and Katsumoto, M.: A study of trajectory quality using methane measurements from Hateruma island, *Atmos. Environ.*, 37, 1911–1919, doi:10.1016/S1352-2310(03)00048-7, 2003.

Atmospheric O₂ and CO₂ changes of pollution events in East Asia

C. Minejima et al.

Title Page

Abstract

Introduction

Conclusions

References

Tables

Figures

⏪

⏩

◀

▶

Back

Close

Full Screen / Esc

Printer-friendly Version

Interactive Discussion

Atmospheric O₂ and CO₂ changes of pollution events in East Asia

C. Minejima et al.

[Title Page](#)
[Abstract](#)
[Introduction](#)
[Conclusions](#)
[References](#)
[Tables](#)
[Figures](#)
[Back](#)
[Close](#)
[Full Screen / Esc](#)
[Printer-friendly Version](#)
[Interactive Discussion](#)


Table 1. Summary of the average $-\Delta\text{O}_2/\Delta\text{CO}_2$ ratios for the individual air mass origins and $-\text{O}_2:\text{CO}_2$ ratios for the corresponding countries

Air mass origin	$-\Delta\text{O}_2/\Delta\text{CO}_2^{\text{a}}$			$-\text{O}_2:\text{CO}_2^{\text{b}}$
	Observation	FLEXPART	coupled model	CDIAC
China	1.14±0.12 (25)	1.08±0.10 (14)	1.07±0.11 (14)	1.11±0.03
Japan/Korea	1.37±0.15 (16)	1.09±0.14 (13)	1.19±0.15 (13)	1.36±0.02
Other	1.20±0.20 (26)	1.15±0.16 (14)	1.18±0.18 (14)	1.45±0.02

^a Uncertainties correspond to the standard deviations. Numbers in the parentheses represent numbers of events.

^b Uncertainties correspond to propagated errors of the $-\text{O}_2:\text{CO}_2$ exchange ratios for individual fuel type and national fossil carbon emissions. The $-\text{O}_2:\text{CO}_2$ exchange ratios for coal, liquid fuel, natural gas burning and gas flaring are 1.17±0.03, 1.44±0.03, 1.95±0.04, and 1.98±0.07, respectively (Keeling, 1988). For the uncertainties associated with the national fossil carbon emissions, ±15% is used for China (Gregg et al., 2008) and ±6% is used for the other countries (Marland and Rotty, 1984).

Atmospheric O₂ and CO₂ changes of pollution events in East Asia

C. Minejima et al.

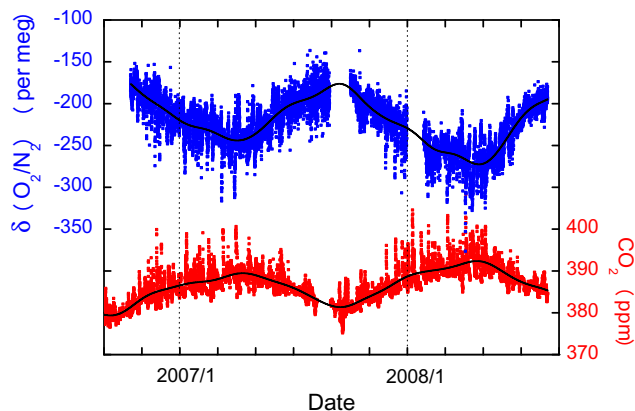


Fig. 1. Time series of atmospheric (blue) O₂/N₂ ratio and (red) CO₂ mole fraction observed at HAT for whole period of this study. Each dot represents hourly average. The smooth curve fits to the data are shown as solid lines.

[Title Page](#)[Abstract](#)[Introduction](#)[Conclusions](#)[References](#)[Tables](#)[Figures](#)[⏪](#)[⏩](#)[◀](#)[▶](#)[Back](#)[Close](#)[Full Screen / Esc](#)[Printer-friendly Version](#)[Interactive Discussion](#)

Atmospheric O₂ and CO₂ changes of pollution events in East Asia

C. Minejima et al.

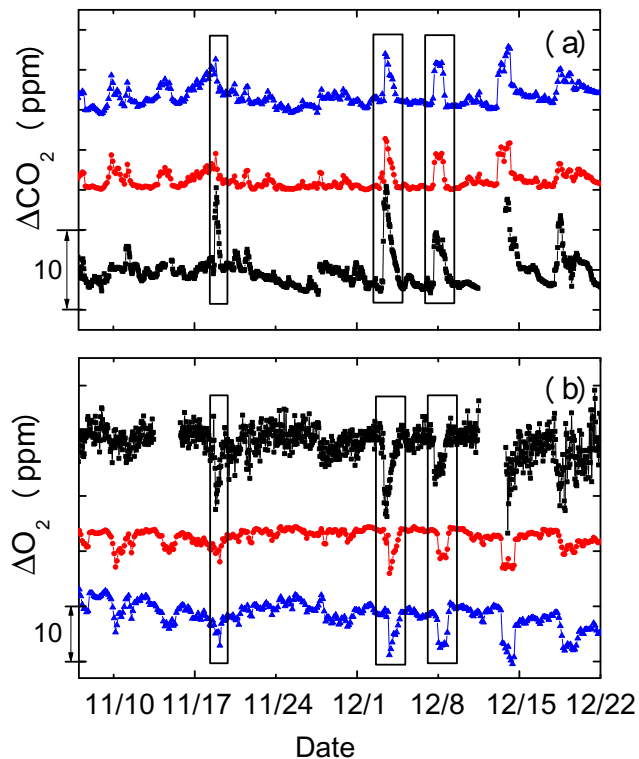


Fig. 2. Short-term variations in (a) ΔCO_2 (ppm) and (b) ΔO_2 (ppm) for the 1-month period (mid November to mid December, 2007). Each dot represents hourly average. Black squares are observations, red circles are model simulation by FLEXPART and blue triangles are model simulation by the coupled model. Pollution events analyzed in this study are enclosed with the black rectangulars.

[Title Page](#)[Abstract](#)[Introduction](#)[Conclusions](#)[References](#)[Tables](#)[Figures](#)[◀](#)[▶](#)[◀](#)[▶](#)[Back](#)[Close](#)[Full Screen / Esc](#)[Printer-friendly Version](#)[Interactive Discussion](#)

Atmospheric O₂ and CO₂ changes of pollution events in East Asia

C. Minejima et al.

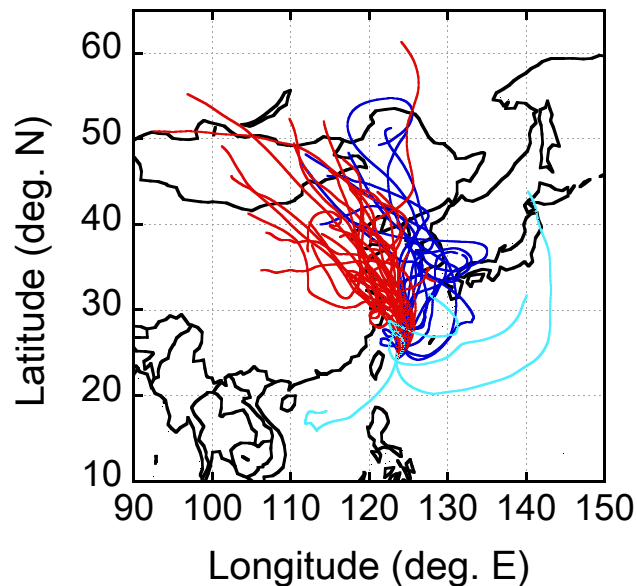


Fig. 3. Five-day back trajectories observed at HAT. The air mass origins are categorized into three regions: China (Red), Japan/Korea (Blue) and Other (Cyan). All events from China and Japan/Korea are depicted and four events from Other are drawn as examples.

[Title Page](#)[Abstract](#)[Introduction](#)[Conclusions](#)[References](#)[Tables](#)[Figures](#)[◀](#)[▶](#)[◀](#)[▶](#)[Back](#)[Close](#)[Full Screen / Esc](#)[Printer-friendly Version](#)[Interactive Discussion](#)

Atmospheric O₂ and CO₂ changes of pollution events in East Asia

C. Minejima et al.

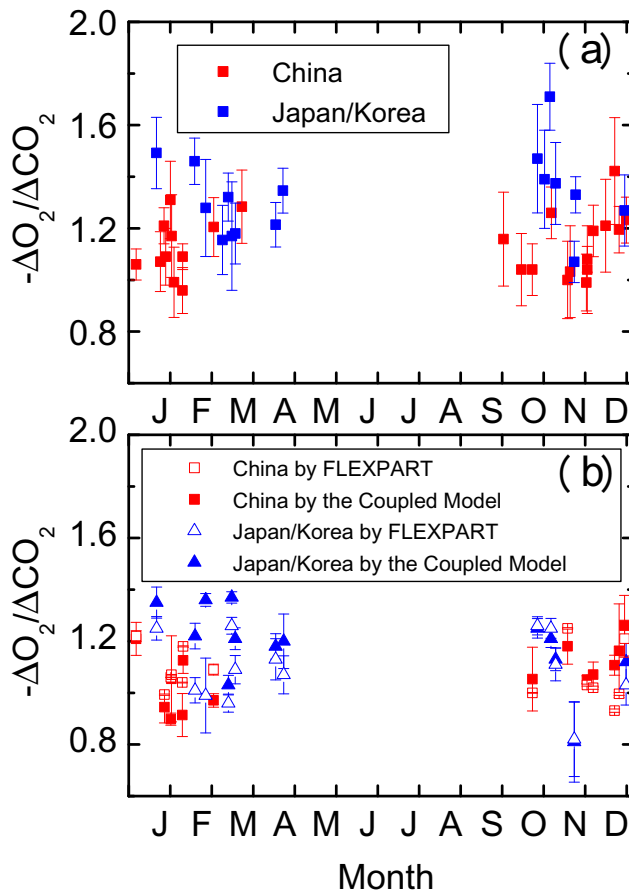


Fig. 4. Calculated regression slope ($-\Delta\text{O}_2/\Delta\text{CO}_2$ ratio) of each pollution event for **(a)** observation and **(b)** model simulations. Red and blue symbols are for events from China and Japan/Korea, respectively. In **(b)**, open symbols are based on FLEXPART and closed symbols are based on the coupled model.

[Title Page](#)
[Abstract](#)
[Introduction](#)
[Conclusions](#)
[References](#)
[Tables](#)
[Figures](#)
[Back](#)
[Close](#)
[Full Screen / Esc](#)
[Printer-friendly Version](#)
[Interactive Discussion](#)

Atmospheric O₂ and CO₂ changes of pollution events in East Asia

C. Minejima et al.

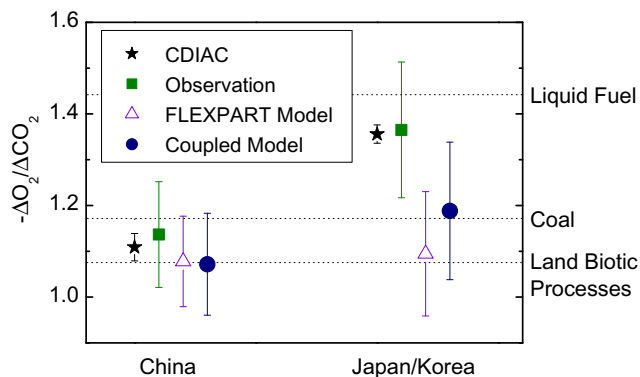


Fig. 5. $-\text{O}_2:\text{CO}_2$ exchange ratios for the fossil carbon emissions from China and Japan/Korea, and average $-\Delta\text{O}_2/\Delta\text{CO}_2$ ratios for the China and Japan/Korea pollution events based on the observations and model simulations using FLEXPART and the coupled model. The national emission inventories of the fossil carbon from the CDIAC database are used to calculate the $-\text{O}_2:\text{CO}_2$ exchange ratios. The vertical bar of CDIAC is the same as Table 1. The standard deviations are shown as vertical bars for observation, FLEXPART Model and Coupled Model. Dotted black lines show estimated $-\text{O}_2:\text{CO}_2$ exchange ratios for land biotic processes (Severinghaus, 1995), coal, and liquid fuel burning (Keeling, 1998).

[Title Page](#)
[Abstract](#)
[Introduction](#)
[Conclusions](#)
[References](#)
[Tables](#)
[Figures](#)
[◀](#)
[▶](#)
[◀](#)
[▶](#)
[Back](#)
[Close](#)
[Full Screen / Esc](#)
[Printer-friendly Version](#)
[Interactive Discussion](#)

Atmospheric O₂ and CO₂ changes of pollution events in East Asia

C. Minejima et al.

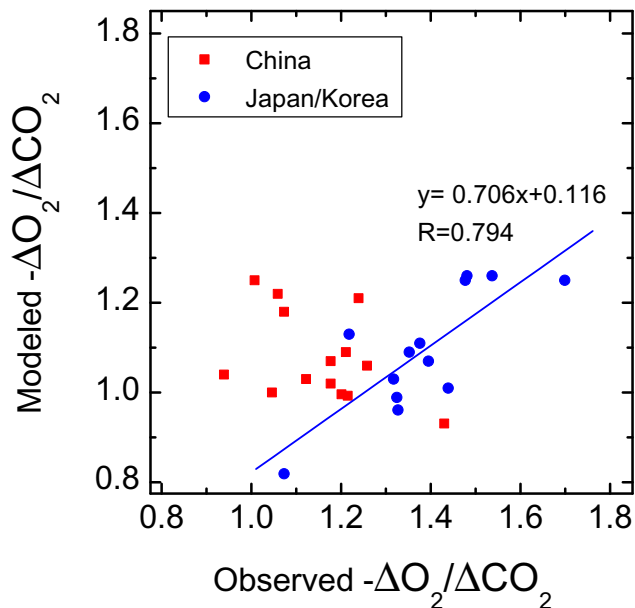


Fig. 6. Scatter plots of the $-\Delta\text{O}_2/\Delta\text{CO}_2$ ratios simulated by FLEXPART model simulation vs. the observation for the events from China and Japan/Korea. Red squares are the events from China and the blue circles are the events from Japan/Korea.

[Title Page](#)[Abstract](#)[Introduction](#)[Conclusions](#)[References](#)[Tables](#)[Figures](#)[◀](#)[▶](#)[◀](#)[▶](#)[Back](#)[Close](#)[Full Screen / Esc](#)[Printer-friendly Version](#)[Interactive Discussion](#)

Atmospheric O₂ and CO₂ changes of pollution events in East Asia

C. Minejima et al.

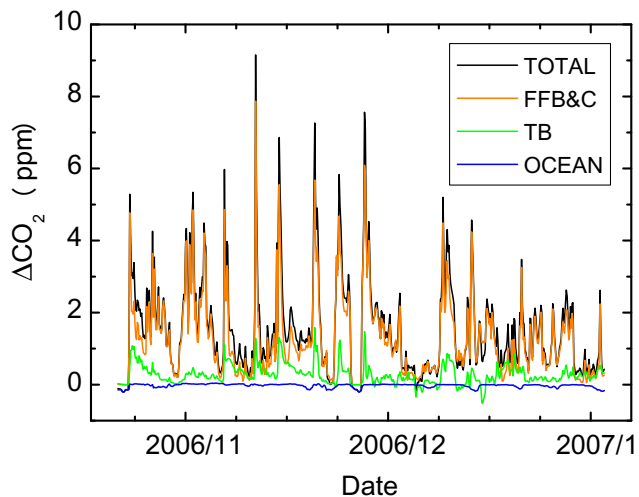


Fig. 7. Components of the ΔCO_2 variation at HAT calculated by FLEXPART. Black line is the total amount of CO_2 from the following three components, orange line is the amount of CO_2 from fossil fuel burning and cement production (FFB&C), green line is from terrestrial biosphere (TB), and blue line is from the ocean.

[Title Page](#)[Abstract](#)[Introduction](#)[Conclusions](#)[References](#)[Tables](#)[Figures](#)[◀](#)[▶](#)[◀](#)[▶](#)[Back](#)[Close](#)[Full Screen / Esc](#)[Printer-friendly Version](#)[Interactive Discussion](#)

Atmospheric O₂ and CO₂ changes of pollution events in East Asia

C. Minejima et al.

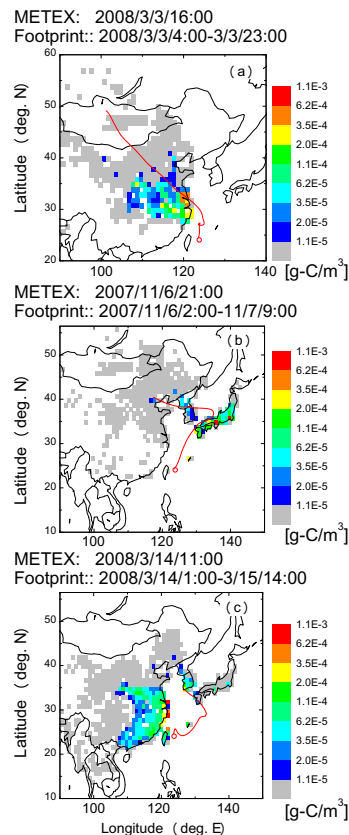


Fig. 8. Footprint for HAT calculated by FLEXPART for the cases in which air mass origins are assigned to **(a)** China, and **(b, c)** Japan/Korea by back trajectory analysis. **(b)** and **(c)** are the cases with small and large Chinese influence, respectively. Color scale is logarithmic. The red lines represent 5-day back trajectories calculated by METEX.

[Title Page](#)
[Abstract](#)
[Introduction](#)
[Conclusions](#)
[References](#)
[Tables](#)
[Figures](#)
[Back](#)
[Close](#)
[Full Screen / Esc](#)
[Printer-friendly Version](#)
[Interactive Discussion](#)